Biosensors and Bioelectronics 312 (2026) 119048



Contents lists available at ScienceDirect

Biosensors and Bioelectronics

journal homepage: www.elsevier.com/locate/bios



Chemical additives-enhanced CRISPR/Cas12a-based RNA detection

Jun Chen [a], Haiyan Zheng [a], Lucas Guan [b], Anudha Kanaherarachchi [a], Sathishkumar Munusamy [a], Juanhua Kong [a], Shuo Zhou [a], Rana Jahani [a], Xiyun Guan [a,*]

[a] Department of Chemistry, University of Missouri, Columbia, MO, 65211, United States
[b] Rock Bridge High School, Columbia, MO, 65203, United States

ARTICLE INFO

Keywords:
Chemical additives
CRISPR/Cas12a
RNA
DNA
Amplification-free detection

ABSTRACT

The CRISPR/Cas12a system has revolutionized molecular diagnostics due to its RNA-guided *trans*-cleavage activity, enabling programmable and highly accurate nucleic acid detection. However, most Cas12a-based assays are optimized for DNA targets, while direct RNA detection constrained by limited sensitivity, typically at the nanomolar level. Existing strategies to improve the performance of RNA analysis often rely on additional DNA activators or complex auxiliary systems. Here, we report a simple yet effective chemical additive-based strategy that overcomes these limitations. This chemical additives-enhanced CRISPR/Cas12a-based RNA detection (CARD) enables femtomolar-level RNA detection using only a single crRNA, without the need for DNA activators, reverse transcription, or strand-displacement reactions. Notably, this approach can be adapted to single-stranded DNA, enabling ssDNA detection at attomolar levels. Collectively, CARD provides a straightforward, amplification-free, and highly sensitive diagnostic framework that might be readily extended to other CRISPR/Cas systems for ultrasensitive nucleic acid diagnostics.

1. Introduction

Clustered regularly interspaced short palindromic repeats (CRISPR)-based systems have emerged as powerful tools for programmable nucleic acid recognition and diagnostics (Jiao et al., 2021; Kaminski et al., 2021). Among them, Cas12a has attracted particular interest because of its strong *trans*-cleavage activity, simple guide RNA design, and inherent signal amplification capability (Broughton et al., 2020; Li et al., 2018; Nguyen et al., 2022; Zetsche et al., 2020; Zhang et al., 2021b). These features have enabled the development of sensitive and robust DNA detection strategies that often require minimal instrumentation (Chen et al. 2018, 2025; Munusamy et al., 2025; Xiong et al., 2020). Although Cas12a ribonucleoproteins can, in principle, recognize RNA, direct RNA detection remains challenging because RNA binding induces only weak *trans*-cleavage activity, leading to poor detection sensitivity (usually at nanomolar levels as demonstrated by the UNIVERSE assay) (Deng et al., 2024; Zhang et al., 2024). Consequently, most CRISPR/Cas12a-based RNA analysis relies on additional processing or amplification steps, such as reverse transcription or strand-displacement reactions to improve the sensing performance (Feng et al., 2021; Wang et al., 2022; Zhang et al., 2021a). RNA-specific CRISPR enzymes, such as Cas13 variants, have been extensively developed for RNA detection; however, they do not directly enable DNA sensing (Rananaware et al., 2023). Furthermore, the RNA reporters commonly employed in Cas13-based assays are generally less stable and more vulnerable to degradation than DNA reporters, resulting in greater challenges for reagent storage, handling, and assay robustness. To date, no CRISPR system can natively detect both DNA and RNA via *trans*-cleavage (Rananaware et al., 2023), and direct RNA sensing with unmodified Cas12a remains rare, underscoring the need for simpler RNA detection platforms.

Recently, several strategies have been developed to overcome the intrinsically weak RNA-mediated activation of Cas12a by engineering nucleic acid interactions. These include SAHARA, which uses a short dsDNA activator targeting the seed region (Gorski et al., 2017; Kim et al., 2020; Swarts and Jinek, 2019; Swarts et al., 2017) to enable one-step RNA detection (Rananaware et al., 2023), FCAS, which exploits fragmented ssDNA activators to achieve femtomolar sensitivity and miRNA imaging (Zhao et al., 2024), and the PHD strategy, which enables Cas12a recognition of ultrashort and structurally complex RNAs (Qiao et al., 2025). More recently, with the help of a ssDNA activator, split crRNA-based designs successfully accomplish direct RNA detection by

* Corresponding author.
E-mail address: xgpc2@missouri.edu (X. Guan).

https://doi.org/10.1016/j.bios.2026.119048
Received 4 May 2026; Received in revised form 16 July 2026; Accepted 18 July 2026
Available online 21 July 2026
0956-5663/© 2026 Elsevier B.V. All rights are reserved, including those for text and data mining, AI training, and similar technologies.

Cas12a without amplification (Chen et al., 2024; Fei et al., 2025; Hu et al., 2025; Jiang et al., 2025; Zhang et al., 2025). To amplify detection signals, asymmetric CRISPR systems based on competitive crRNA binding (Moon et al., 2025) and autocatalytic Cas12a activation via circular DNA linearization (AutoCAR) (Deng et al., 2024) have also been reported. Although engineering nucleic acid interactions could enhance Cas12a activation for RNA sensing, the reliance on additional DNA activators, complex hybrid architectures, or multicomponent designs increases experimental complexity and limits practical usability. The performance comparison of various existing RNA detection approaches was summarized in Supplementary Table S1.

Here, we report that simple chemical additives can substantially enhance the intrinsic RNA-triggered *trans*-cleavage activity of Cas12a (Fig. 1). This additive-enabled strategy markedly improves RNA detection sensitivity and significantly outperforms previously reported direct RNA detection methods (nanomolar sensitivity) (Li et al., 2022; Zhang et al., 2024), enabling robust detection at the femtomolar level. Moreover, the same chemical additive strategy can be adapted to single-stranded DNA. Remarkably, under the optimized conditions, attomolar concentrations of DNA could be detected. Collectively, our findings reveal a simple yet highly powerful method for enhancing Cas12a *trans*-cleavage activity, advancing both mechanistic studies of Cas12a biochemistry and the development of ultrasensitive nucleic acid detection platforms.

2. Materials and methods

2.1. Materials and reagents

LbCas12a and the FAM-labelled ssDNA reporter probes, along with the DNA and RNA oligonucleotides listed in Supplementary Table S2, were ordered from Integrated DNA Technologies (Coraville, IA, USA). The 10 × NEbuffer 2.1 was obtained from New England Biolabs (Ipswich, MA). All the other chemicals used in this work were purchased from Sigma-Aldrich (St. Louis, MO). Ultrapure water was used throughout the experiments. All DNA oligonucleotides and RNA samples were dissolved in DNase-free, RNase-free water and stored at −20 °C before and immediately after experiments.

2.2. Preparation of Cas12a-crRNA analysis system (**Component A**, final volume is 50 μL)

The Cas12a-crRNA analysis system was prepared by combining 27 μL of HPLC-grade water, 5 μL of 10× NEbuffer 2.1, 4 μL of LbCas12a (200 nM), 4 μL of crRNA (100 nM), and 10 μL of ssDNA reporter (5 μM). The mixture was incubated at 25 °C for 15 min to prepare Component A.

2.3. Preparation of reaction media for detergent and small-molecule additive screening (**Component B**, final volume is 100 μL)

Detergent screening and small-molecule additive optimization were conducted in a stepwise manner to ensure controlled buffer composition during each screening stage.

2.4. Detergent screening

The stock solutions of detergents were prepared in reaction buffer (1x NEbuffer 2.1) at concentrations of 1% (v/v), 1% (v/v), 1% (v/v), 10 mM, 1 mM and 100 μM for Tween 20, Triton X-100, IGEPAL CA-630, Brij 35, PVP, and SDS, respectively. Reaction media were then prepared by serial dilution of these stock solutions to the desired final detergent concentrations to make the Component B.

2.5. Small-molecule additive screening (DTT and L-proline)

Stock solutions (at 40 mM and 100 mM concentrations, respectively) of DTT and L-proline were prepared in reaction buffer supplemented with 0.1% (v/v) Tween 20. Serial dilutions were subsequently carried out using the same reaction buffer containing 0.1% (v/v) Tween 20 to generate Component B.

2.6. Preparation of glycerol-containing reaction media

For experiments involving glycerol, reaction media were prepared by volumetric mixing of glycerol with reaction buffer containing 0.1% (v/v) Tween 20. The final volume of the reaction medium was fixed at 100 μL. At the optimal glycerol condition (50% v/v), the reaction medium consisted of 50 μL glycerol and 50 μL of reaction buffer supplemented with 0.1% (v/v) Tween 20. As a result, the effective buffer component concentration was reduced proportionally due to the large volume fraction of glycerol.

Unless otherwise stated, the concentrations of detergents and small-molecule additives reported in this study were calculated based on the preparation of reaction media at a fixed total volume of 100 μL, rather than their effective concentrations after subsequent mixing with component A.

The RNA-optimized reaction medium was prepared by mixing equal volumes of glycerol and reaction buffer supplemented with 0.1% (v/v) Tween 20, resulting in a reaction medium containing 50% (v/v) glycerol.

The DNA-optimized reaction medium consisted of reaction buffer supplemented with 0.1% (v/v) Tween 20.

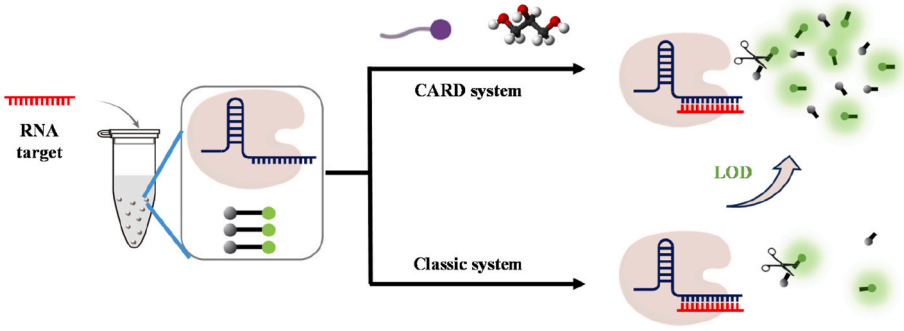


Fig. 1. Schematic illustration of the chemical additives-enhanced CRISPR/Cas12a biosensing platform. In the conventional system (without chemical additives), target RNA hybridizes with the guide RNA, inducing relatively weak Cas12a *trans*-cleavage activity. This limited *trans*-cleavage of fluorophore-quencher–labelled single-stranded DNA (ssDNA) reporters produces low fluorescence intensity, resulting in poor detection sensitivity. In contrast, in the presence of chemical additives (CARD assay), target RNA recognition markedly enhances Cas12a *trans*-cleavage activity, leading to more efficient reporter cleavage, significantly increased fluorescence signals, and improved biosensing performance.

2.7. Electrical recordings and data analysis of nanopore results

Nanopore single-channel recordings and data analysis were conducted following the procedure described in detail in our previous work (Zheng et al., 2025). The $(M117F)_7$ α-hemolysin protein was used as the nanopore sensing element, which was added to the grounded *cis* chamber compartment. The ssDNA reporter or its mixture was also added to the *cis* compartment after a single channel was formed. The ssDNA reporter mixture samples were prepared by incubating HPLC-grade water (22 μL), 10× NEbuffer 2.1 (5 μL), LbCas12a (4 μL, 200 nM), and crRNA (4 μL, 100 nM) at 25 °C for 15 min. Then, ssDNA reporter (15 μL, 100 μM), 100 μL of reaction buffer or RNA-optimized reaction medium, and 4 nM RNA-1 were added, followed by incubation at 37 °C for 2 days. After that, the mixture solutions were heated at 60 °C for 10 min to denature LbCas12a and terminate the reaction.

2.8. Fluorescence assay for RNA detection

Fluorescence measurement was performed using the Shimadzu RF6000 Fluorometer System (Bio-Rad, CA, USA). Briefly, the LbCas12a-crRNA analysis system was first prepared and incubated to allow formation of Component A. Subsequently, 100 μL of RNA-optimized reaction medium (Component B) and RNA analytes at various concentrations were added, followed by incubation at 37 °C for 3 h. After heating at 60 °C for 5 min to denature LbCas12a and terminate the reaction, fluorescence was then measured at λex/λem = 480/521 nm.

2.9. Fluorescence assay for DNA detection

Similar to RNA detection, the LbCas12a-crRNA analysis system was first prepared and incubated to allow formation of Component A. Subsequently, 100 μL of DNA-optimized reaction medium (Component B) and DNA analytes at various concentrations were added, followed by incubation at 47 °C for 3 h. After the reaction, the sample was heated at 60 °C for 5 min to denature LbCas12a and terminate the reaction. Fluorescence was then measured at λex/λem = 480/521 nm.

2.10. Serum Sample Analysis

Human male AB plasma (U.S. origin; Sigma-Aldrich, St. Louis, MO, USA) was used as a representative biological matrix. RNA was extracted from 200 μL of serum using the miRNeasy Serum/Plasma Advanced Kit (Qiagen, Cat. No. 217204) according to the manufacturer's instructions. The extracted RNA was analyzed using the optimized CRISPR-Cas12a assay. For spike-and-recovery experiments, three mock serum samples were prepared by spiking synthetic miRNA-21 into serum at three concentration levels prior to RNA extraction and analyzed following the same procedure.

2.11. Limit of detection calculation

The LOD was determined by conducting the *trans*-cleavage assays using RNA or DNA standard solutions with varying concentrations. After constructing the linear relationships between the fluorescence intensity and the RNA/DNA concentration, the LOD value was calculated by using formula 3σ/slope, where σ is the standard deviation of three blank solutions.

2.12. Statistics and reproducibility

No statistical method was used to pre-determine sample size. Unless otherwise stated, all experiments were conducted in a minimum of three independent experimental batches or in three independent replicates to assess reproducibility. No data were excluded from the analyses. The experiments were not randomized, and the investigators were not blinded during experiments and outcome assessment. Quantitative data are reported as the mean ± standard deviation (SD), as specified in the corresponding figure legends. Statistical analyses were performed using OriginLab software. Comparisons between two independent groups were evaluated using two-tailed independent samples t-tests. A p-value <0.05 was considered statistically significant. Detailed statistical information, including the statistical test used, exact p-values, sample size (n), and other relevant parameters, is provided in the corresponding figure legends.

3. Results

3.1. Investigating the effects of chemical additives on Cas12a-based RNA detection

Due to their ability to stabilize proteins and modulate solvent properties, thereby influencing reaction kinetics, a wide range of chemicals have been utilized as effective solvent additives to enhance the performance of biosensing, including sensitivity, selectivity and stability. Although such additives have been explored to enhance CRISPR-based DNA detection, their potential to improve RNA analysis remains largely underexploited (Cai et al., 2017; Feng et al., 2023; Li et al., 2021; Lin et al., 2022; Liu et al., 2024; Ma et al., 2020). To address this gap, we first evaluated the feasibility of using solvent additives to enhance the sensitivity of Cas12a-mediated RNA detection. A 22-nucleotide RNA oligonucleotide (RNA-1; sequence: 5′-rCrCrC rArGrG rUrArA rArCrA rCrArC rArArA rCrCrU rU-3′) was selected as a model target. Among potential additives, surfactants are particularly attractive for biosensing applications due to their low cost, biocompatibility, and documented ability to minimize nonspecific adsorption, inhibit protein aggregation, and maintain the conformation of enzymes (Liu et al., 2024; Qing et al., 2025). Accordingly, we systematically investigated the effects of surfactant type and concentration on the detection of RNA-1 (Fig. 2A). We found that, nonionic surfactants like Tween 20 (Fig. 2B), Triton X-100 (Fig. 2C), IGEPAL CA-630 (Fig. 2D), and Brij 35 (Fig. 2E) remarkably enhanced the Cas12a *trans*-cleavage activity within a certain concentration range, as demonstrated by the significantly boosted fluorescence signal of the RNA-1 solution and signal-to-noise (S/N) ratio (Fig. 2H), indicating improved accessibility of the RNA-1 substrate and stabilization of the Cas12a-crRNA-target complex under mild conditions (Qing et al., 2025). In contrast, PVP, the polymeric additive that has been used in enhanced CRISPR-Cas systems for robust DNA diagnostics (Liu et al., 2024; Qiao et al., 2025), showed negligible influence on Cas12a activity in all tested concentrations in our RNA-1 detection system (Fig. 2F and H), while ionic detergent SDS strongly suppressed fluorescence generation at high concentrations (Fig. 2G and H), probably due to the electrostatic interaction between the ionic surfactants and the CRISPR/Cas12a mixture (Liu et al., 2024). Among various surfactants, 0.1% Tween 20 showed the highest fluorescence signal and the largest S/N ratio, and hence was deemed as the optimum surfactant condition and used in the remaining experiments.

Besides surfactants, functional small molecules have also been scrutinized for improving and/or modulating CRISPR assay efficiency. For instance, DTT is a widely used additive in CRISPR-based analysis, which can not only relax the PAM base-pairing requirements for LbCas12a, thereby expanding targetable loci (Qing et al., 2025), but also enhance *trans*-cleavage activity (Deng et al., 2022). Moreover, Li et al., (2021) found that L-proline stabilizes or improves the DNA detection ability of Cas12a/Cas13a, while Lin et al., (2022) discovered that glycerol greatly improved the efficacy of a one-pot RPA CRISPR/Cas12a assay. Inspired by these findings, we next investigated the hypothesis that supplementation of the Tween 20-containing reaction buffer with additional chemical regents such as DTT, L-proline or glycerol might further enhance the sensitivity of the CRISPR/Cas12a system for RNA-1 detection (Fig. 3A). Unexpectedly, the three chemicals showed markedly different effects. Specifically, although the fluorescence intensity of the RNA-1 sample increased as the DTT concentration was raised from

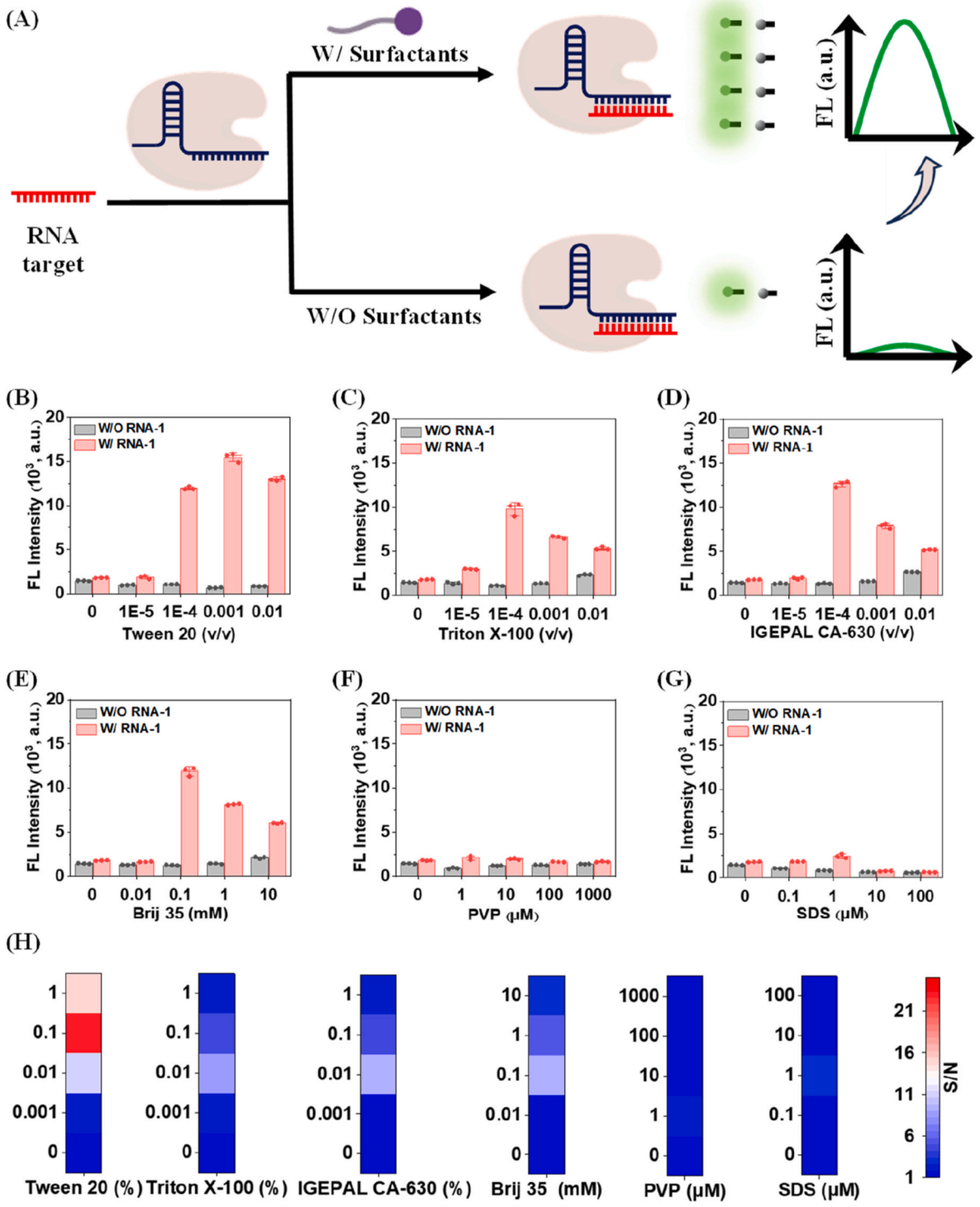


Fig. 2. Evaluation of the effects of surfactants on CRISPR-Cas12a based RNA detection. (A) Schematic representation of surfactant-enhanced Cas12a *trans*-cleavage of dye-labelled ssDNA reporters, triggered by the target RNA. Plots of fluorescence intensity versus surfactant concentration and species: (B) Tween 20, (C) Triton X-100, (D) IGEPAL CA-630, (E) Brij 35, (F) PVP, and (G) SDS. (H) The corresponding heat maps of signal to noise (S/N) ratio, where S represents the fluorescence intensity of the RNA sample, while N represents fluorescence intensity of the control. The fluorescence measurement was performed with λex/λem = 480/521 nm. The incubation was performed at 37 °C for 1 h in reaction buffer supplemented with different detergent species of varying concentrations. The error bars indicate the average and standard deviation values derived from results obtained in three independent experiments (n = 3). The concentration of RNA-1 used in Fig. 2 was 2 nM each.

40 μM to 4 mM, the background fluorescence level increased more significantly, leading to a reduction in the S/N ratio compared to the DTT-free condition (Fig. 3B). In contrast, L-proline did not improve RNA-1 detection performance, as demonstrated by the stable fluorescence intensity and the S/N ratio when the L-proline concentration varied from 100 μM to 10 mM, while a further increase in its concentration led to a slight decrease in both the parameters (Fig. 3C). Regarding glycerol, as its proportion (v/v) in the reaction buffer

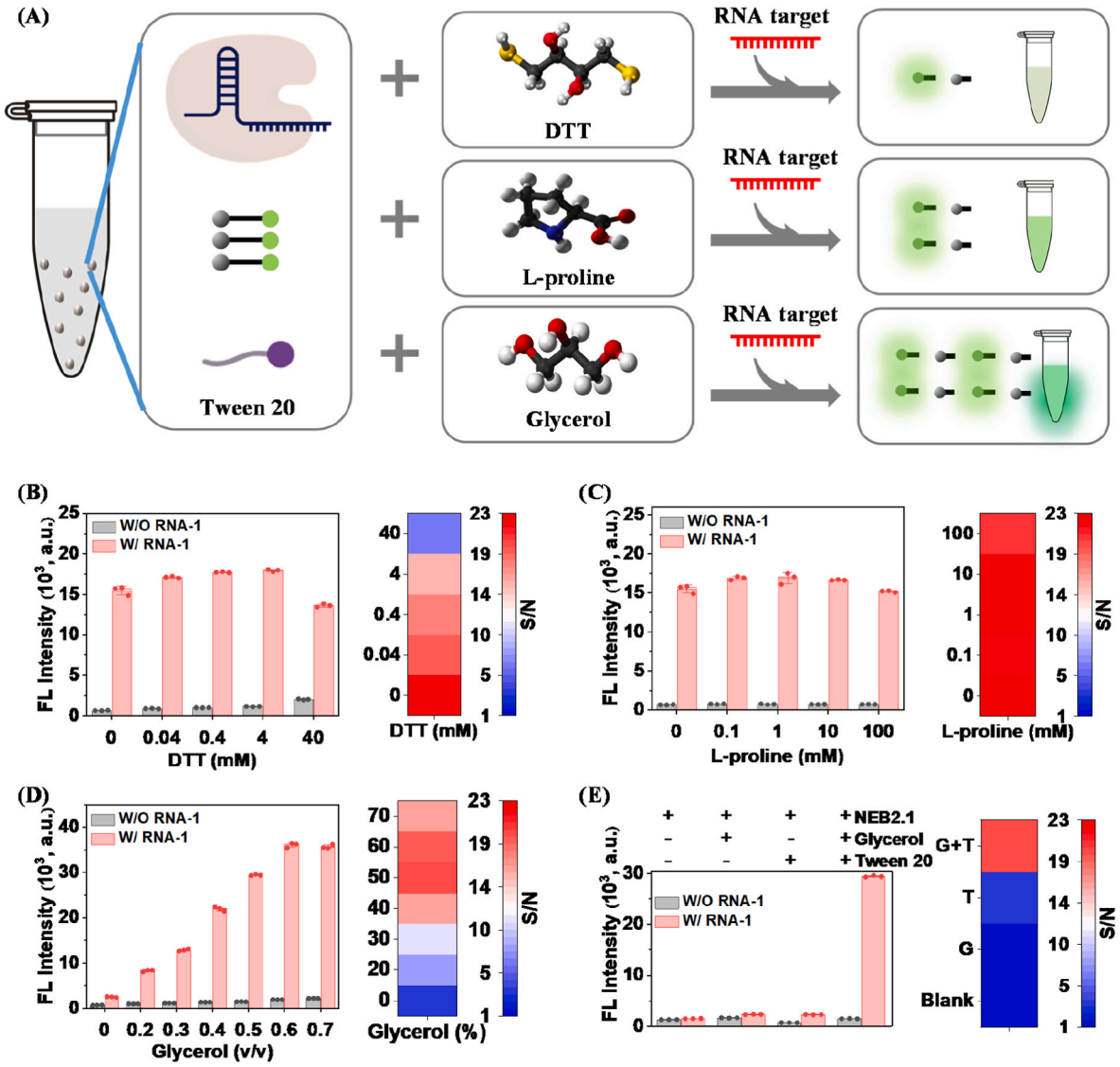


Fig. 3. Study of the effects of functional small molecules on RNA detection. (A) Schematic representation of small molecule-enhanced Cas12a *trans*-cleavage of dye-labelled ssDNA reporters, triggered by the target RNA. Plots of (*left*) fluorescence intensity and (*right*) the corresponding heat map of S/N ratio as a function of chemical concentration and species: (B) DTT, (C) L-proline, (D) glycerol. (E) The effect of buffer components on RNA detection. The fluorescence measurement was performed with λex/λem = 480/521 nm. In Fig. 3B–D, the reaction buffer was supplemented with 0.1% (v/v) Tween 20. The incubation was performed at 37 °C for 1 h. The error bars indicate the average and standard deviation values derived from results obtained in three independent experiments (n = 3). The concentrations of RNA-1 used in Fig. 3B–C were 2 nM each, while those of RNA-1 in Fig. 3D–E were 200 pM each.

increased, the fluorescence signal of the RNA-1 solution increased substantially, while the background fluorescence only increased slightly (Fig. 3D). Consequently, the S/N ratio reached a maximum at a glycerol proportion of 50% (v/v). Further elevating the glycerol level led to a decreasing S/N value (Fig. 3D), and hence 1:1 vol mixture of glycerol and reaction buffer supplemented with 0.1% (v/v) Tween 20 was chosen as the RNA-optimized reaction medium. Taken together, the combined results suggest that, under our experimental conditions, the effect of L-proline on Cas12a-based RNA-1 detection was negligible, while DTT and glycerol would significantly decrease and increase the sensitivity of RNA-1 detection, respectively.

3.2. *Investigation of the mechanism behind chemical enhancement of CRISPR/Cas12a-based RNA analysis*

To gain insight into the mechanism by which the glycerol/Tween 20 mixture markedly enhances CRISPR/Cas12a-based RNA-1 detection, a series of mechanistic experiments was carried out. We first investigated the individual and combined effects of glycerol and Tween 20 by comparing four reaction buffer compositions (Fig. 3E and Fig. S1). We found that, compared with the standard reaction buffer, addition of an equal volume of glycerol produced a slight increase in the fluorescence signal and S/N value, whereas supplementing with 0.1% Tween 20 resulted in a more pronounced improvement (Fig. 3E). Notably, when glycerol and Tween 20 were combined, both the fluorescence signal and S/N value increased dramatically (far exceeding the sum of their individual contributions), indicating a strong synergistic effect (Fig. 3E). This synergistic enhancement might stem from their complementary effects on the local reaction environment, including enhanced fluorophore stability, reduced self-quenching and non-specific interactions, and optimized microviscosity, collectively resulting in brighter and more stable fluorescence signals (Deng et al., 2022; Lin et al., 2022; Liu et al., 2024).

Since addition of glycerol simultaneously diluted the reaction buffer components, we next examined whether the improved assay performance simply resulted from buffer dilution. To test this hypothesis,

glycerol was replaced with an equal volume of water while maintaining the same dilution factor. As a result, both the fluorescence signal and S/N value decreased significantly (Fig. S1). Moreover, compared with the RNA-optimized reaction medium, increasing the concentration of either the reaction buffer or Tween 20, individually or simultaneously, also led to a decrease in the S/N ratio (Fig. S1). These results indicate that the enhanced analytical performance cannot be attributed to dilution alone but instead requires the combined presence of Tween 20 and glycerol.

We next investigated whether the increased fluorescence was due to direct interactions between the additives and the fluorescent reporter. For this purpose, both the quenched and unquenched reporters were incubated in reaction buffers containing different additives in the absence of Cas12a. We found that glycerol alone did not affect the fluorescence of the quenched reporter, while Tween 20 alone enabled an enhanced quenching efficiency of the quenched reporter, as demonstrated by the significantly lower background fluorescence. Although the glycerol/Tween mixture also lowered background fluorescence, the effect was less significant than that of Tween 20 alone (Fig. S2A). In contrast, the fluorescence intensities of the cleaved reporters were essentially identical in the absence and presence of additives (Fig. S2B). These findings indicate that the additives neither induce reporter cleavage nor directly enhance the fluorescence of the released FAM fluorophore.

Having excluded dilution and direct fluorophore effects, we next sought direct evidence that the chemical additives enhance Cas12a *trans*-cleavage activity. To this end, nanopore analysis was carried out to monitor reporter cleavage (Fig. 4). By monitoring ionic current modulations induced by the interaction between target analytes and a nanocavity, nanopore stochastic sensing has emerged as a powerful, versatile tool to explore a wide variety of applications at the single-molecule level (Chen et al., 2023; Li et al., 2025; Sun et al., 2025; Yi et al., 2025). Due to its high sensitivity and excellent resolution, nanopore technology is very useful to study short nucleic acid/peptide cleavage at low concentrations (Zhao et al., 2009; Zheng et al., 2024). We found that, in the absence of Tween 20 and glycerol, the 5-mer ssDNA reporter (FAM-TTATT-IABkFQ) alone generated a broad amplitude distribution, short-lived current blockade events when analyzed using the $(M117F)_7$ α-hemolysin nanopore (Zheng et al., 2026a). The residual current histogram exhibited a dominant I_r/I_o peak at approximately 0.9 (Fig. 4A), indicating transient pore occupancy. A similar result was obtained with the Cas12a/crRNA/RNA-1/ssDNA reporter mixture (Fig. 4B). Notably, the event count corresponding to the major peak remained essentially unchanged, indicating negligible Cas12a activity under these conditions. In contrast, when Tween 20 and glycerol were introduced, the

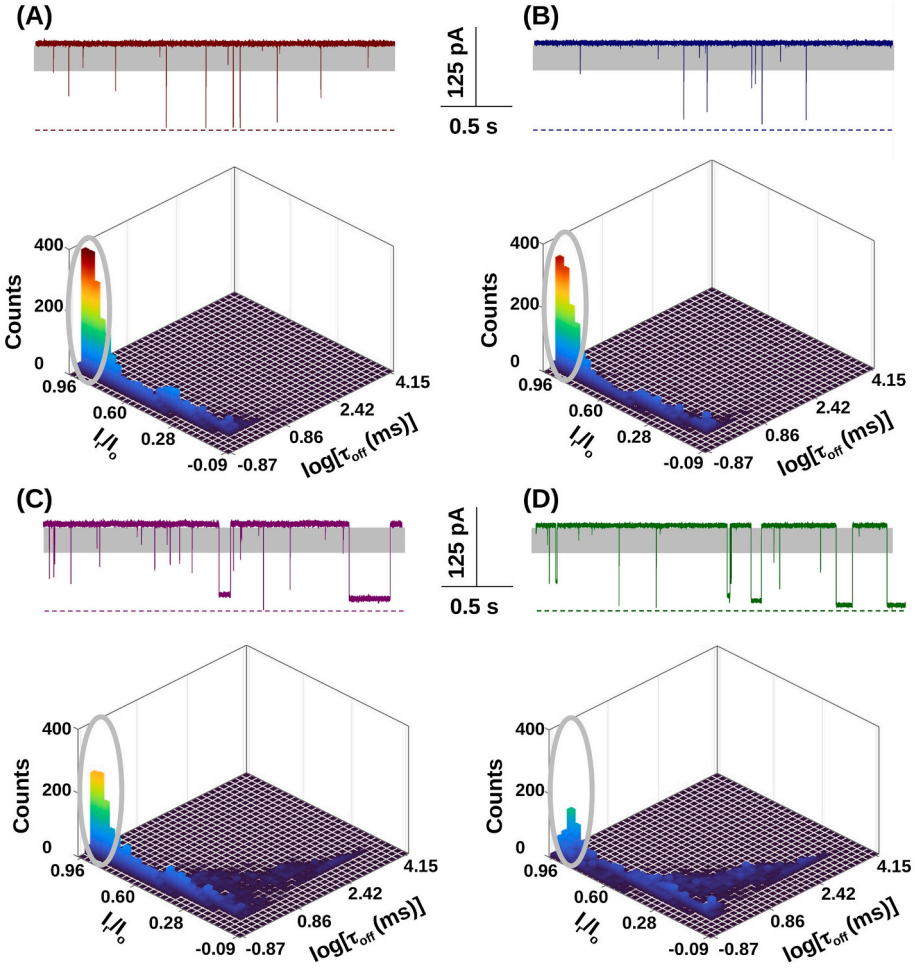


Fig. 4. Nanopore analysis of reporter ssDNA cleavage by Cas12a in the absence and presence of Tween 20 and glycerol. (A) (top) a representative trace segment of ssDNA reporter and (bottom) the corresponding 3D plots of event amplitude versus residence time versus event counts; (B) (top) a representative trace segment of Cas12a/crRNA/RNA-1/ssDNA reporter mixture and (bottom) the corresponding 3D plots of event amplitude versus residence time versus event counts; (C) (top) a representative trace segment of the ssDNA reporter sample containing Tween 20 and glycerol and (bottom) the corresponding 3D plots of event amplitude versus residence time versus event counts; and (D) (top) a representative trace segment of the Cas12a/crRNA/RNA-1/ssDNA reporter mixture containing Tween 20 and glycerol and (bottom) the corresponding 3D plots of event amplitude versus residence time versus event counts. The experiment was carried out at +150 mV in an electrolyte solution containing 1 M NaCl and 10 mM Tris (pH 7.5). The final concentrations of the reporter ssDNA in the mixture or non-mixture samples were 100 nM each. The 3D plots were obtained based on 10 min trace segments.

ssDNA reporter sample exhibited two distinct event populations (Fig. 4C). The short-lived, large-amplitude spread events were attributed to the reporter, whereas the long-lived events were assigned to Tween 20, as confirmed by control experiments (Fig. S3). Importantly, in the Cas12a/crRNA/RNA-1/ssDNA reporter mixture containing Tween 20 and glycerol, the number of events corresponding to the reporter-associated major peak was markedly reduced (Fig. 4D), consistent with efficient reporter cleavage by activated Cas12a. These nanopore measurements provide direct single-molecule evidence that the glycerol/Tween 20 mixture enhances CRISPR/Cas12a assay performance primarily by promoting Cas12a *trans*-cleavage activity rather than by directly affecting the fluorescent reporter.

3.3. Optimization of the incubation parameters to enhance RNA-1 detection

To further improve the sensitivity of the additive-enhanced CRISPR-LbCas12a assay, several key reaction parameters were systematically investigated, including the molar ratio of Cas12a to crRNA, incubation temperature, and incubation time. As shown in Fig. S4A, as the molar ratio of Cas12a to crRNA decreased, both the fluorescence intensity of the RNA-1 sample and the S/N ratio first increased and then decreased,

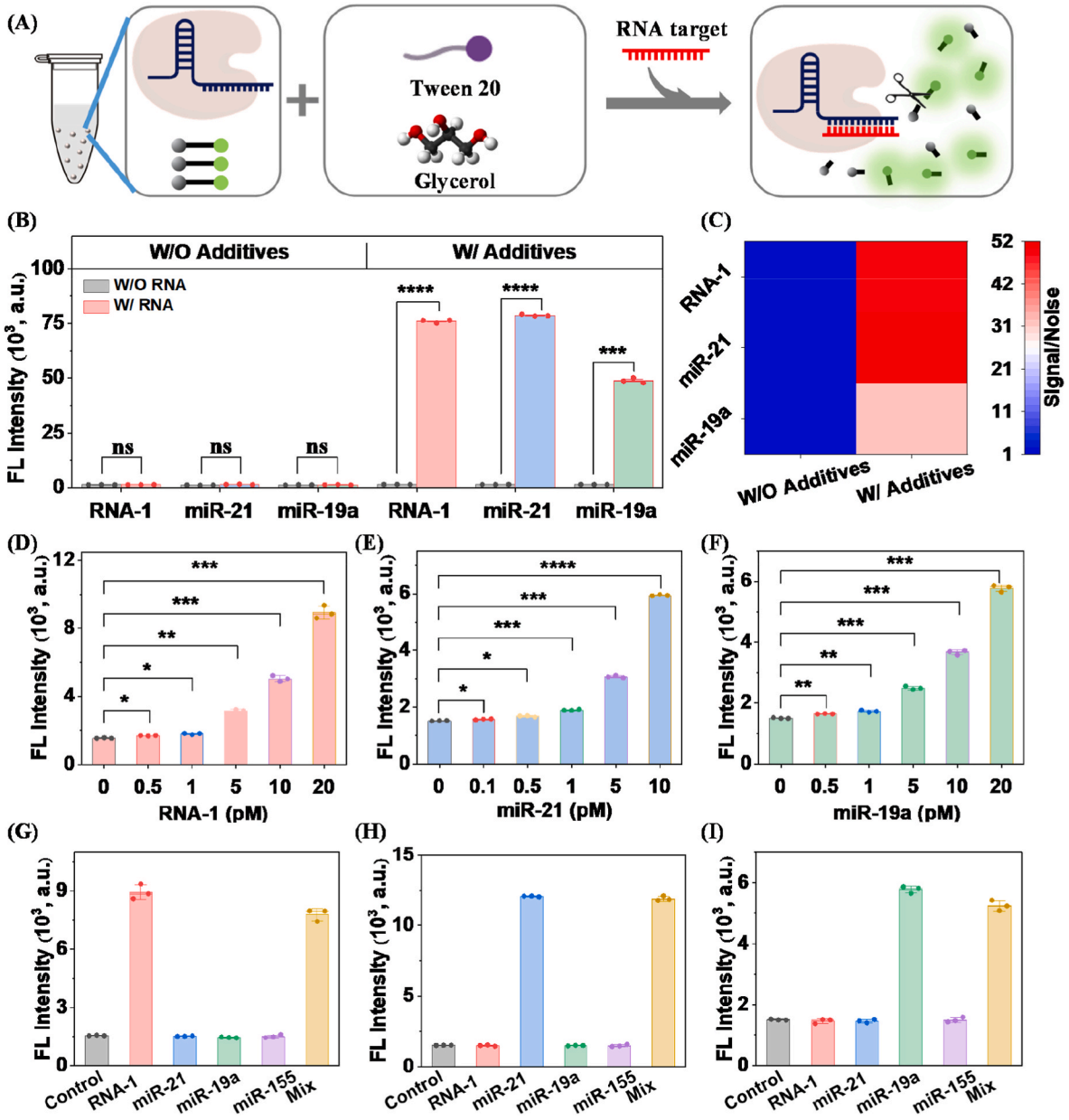


Fig. 5. Chemical additive-enhanced Cas12a assay for the sensitive and efficient detection of various RNA species. (A) Schematic representation of RNA-triggered Cas12a *trans*-cleavage of ssDNA reporters in RNA-optimized reaction medium. (B) The effect of solvent additives on RNA detection and (C) the corresponding heat map of signal to noise ratio. Plots of the fluorescence intensity as a function of the concentration of target RNA: (D) RNA-1; (E) miR-21 and (F) miR-19a. (G-I) Specificity studies. The incubation was performed at 37 °C for 3 h in RNA-optimized reaction medium. The error bars indicate the average and standard deviation values derived from results obtained in three independent experiments (n = 3). Statistical analysis was conducted using a two-tailed *t*-test. Significance levels are indicated as follows: ns (not significant) for $P > 0.05$, * for $P < 0.05$, ** for $P < 0.01$, *** for $P < 0.001$, and **** for $P < 0.0001$. Except the target RNA (i.e., RNA-1, miR-21, and miR-19a in Fig. 5G–I, respectively), whose concentration was at 20 pM each, the concentrations of other non-target RNA species used in Fig. 5G–I were 200 pM each. Each mixture sample contained 20 pM of the target RNA and three other non-target RNA species, each of which was at 200 pM. The corresponding guide RNAs for RNA-1, miR-21, and miR-19a were used in Fig. 5G–I, respectively.

with the optimum ratio observed at 2:1. Temperature effect showed a similar phenomenon, with 37 °C yielding the strongest fluorescence intensity and the largest S/N value (Fig. S4B). In contrast, prolonging the incubation time from 0.5 h to 6 h induced continuous increases in both fluorescence signals and S/N values (Fig. S4C). However, considering practical applications where rapid analysis is preferred, 3 h was chosen as the optimal incubation time for remaining experiments. In addition, we also tested crRNA-7DNA, where a 7-mer DNA extension was appended to the 3′ terminal of the conventional crRNA, and dye-labelled hairpin DNA reporter instead of single-stranded reporter DNA in our system (Fig. S5). Both strategies have been used in the literature to enhance CRISPR/Cas12a *trans*-cleavage activity (Nguyen et al., 2020; Rossetti et al., 2022). However, our experiments showed that the standard crRNA and ssDNA reporter outperformed them in RNA-1 detection.

3.4. Chemical additives-enhanced CRISPR-Cas12a system enables effective detection of various RNA sequences

Having established that combined use of Tween 20 and glycerol could significantly enhance the sensitivity of RNA-1 detection by Cas12a (Fig. 5A), we next investigate the generality of this CARD strategy for RNA analysis by examining two additional cancer-associated miRNA biomarkers, miR-21 and miR-19a. Similar to RNA-1, in the absence of chemical additives, the fluorescence signals obtained from these RNA targets at 200 pM were indistinguishable from the negative control (Fig. 5B and C), consistent with the reported nanomolar detection limit of conventional direct Cas12a-based RNA detection. In contrast, in the presence of Tween 20 and glycerol, these RNA samples produced significantly larger fluorescence intensities than their corresponding controls although the signal to noise ratios differed (ranging from 32 to 52). To evaluate the performance of the chemical additives-enhanced CRISPR-Cas12a system operated under optimized physical conditions, dose-response curves for RNA-1, miR-21 and miR-19a were then constructed. We found that an increase in the RNA-1/miR-21/miR-19a concentration led to an increase in the fluorescence intensity (Fig. 5D–F). Good linear relationships (RNA-1: $y = 345.67x + 1519.17$ and $R^2 = 0.9909$; miR-21: $y = 434.32x + 1508.84$ and $R^2 = 0.9933$; and miR-19a: $y = 211.39x + 1529.07$ and $R^2 = 0.9974$) existed between the fluorescence intensity and the RNA concentration over the entire concentration range examined (Fig. S6–8). The limits of detection (LODs) of the method were determined to be 139 fM, 40 fM and 179 fM for RNA-1, miR-21 and miR-19a, respectively, based on the 3σ criterion (Zheng et al. 2025, 2026b). To examine the feasibility of further improving the sensor sensitivity, miR-21 detection was next performed by extending the incubation time from 3 h to 6 h. We found that the LOD for miR-21 was successfully lowered to 8.09 fM (Fig. S9). Moreover, the selectivity of our developed method was systematically evaluated by assessing its cross-reactivity toward the target RNA in the presence of potential interfering species. The experimental results (Fig. 5G–I) showed that the non-target RNA species having 10-fold higher concentrations than the target analytes in all the three sensing systems produced negligible fluorescence intensities similar to those of the controls, while the corresponding target RNA signals were clearly observed. In addition, to challenge the sensing systems with matrix effects, mixture samples were analyzed, where each mixture sample contained 20 pM of the target RNA and three other non-target RNA species, each of which had a 10-fold concentration than the target analyte. We found that presence of large amount of other RNA molecules would affect the target RNA's signal slightly, possibly because they hindered the binding of the crRNA toward the trace amount of target RNA sequence. Taken together, the combined results demonstrate that our sensing platform is highly selective and suitable for identifying specific miRNA biomarkers within complex RNA pools. Moreover, to evaluate whether the developed CARD-based RNA detection strategy is applicable to other Cas12a orthologs, we investigated AsCas12a. Although the enhancement was less pronounced than that observed for LbCas12a, a substantial improvement in detection performance was still observed (Fig. S10).

3.5. Extending the chemical additives-enhanced CRISPR-Cas12a system for DNA detection

To determine whether the chemical additives-enhanced strategy could be expanded to ultra-sensitive DNA detection, a series of parameters was next systematically optimized, including surfactants (Fig. S11), functional small molecules (Fig. S12), reaction temperature (Fig. S13A), and incubation time (Fig. S13B). We found that reaction buffer supplemented with 0.1% Tween 20 (named DNA-optimized reaction medium) remained the optimal surfactants–buffer combination for detection of a 25-mer model DNA target, DNA-1, with a sequence of 5′- CCC AGG TAA ACA CAC AAA CCT TTT T -3’ (Fig. S11A). However, unlike RNA detection, addition of glycerol in the Tween 20-containing reaction buffer did not improve the sensitivity toward DNA-1 targets (Fig. S12C). Moreover, the optimal incubation temperature shifted from 37 °C for RNA detection to 47 °C for DNA-1 analysis (Fig. S13A). To investigate why glycerol failed to enhance DNA detection sensitivity, we further evaluated its effect in the absence of Tween 20. Interestingly, glycerol alone enhanced RNA detection but reduced the sensitivity of DNA detection (Fig. S14). One possible explanation is that glycerol preferentially stabilizes the crRNA–RNA hybrid, thereby promoting Cas12a activation and subsequent *trans*-cleavage of the ssDNA reporter. In contrast, glycerol may not similarly stabilize the crRNA–DNA hybrid or may even interfere with its formation, resulting in reduced target recognition and diminished Cas12a activity during DNA detection. Using the experimental conditions (DNA-optimized reaction medium, incubation temperature at 47 °C and 3 h incubation time), a series of DNA sequences, which have been widely used in various biosensor applications, was then analyzed by the CRISPR-Cas12a system, where their corresponding guide RNAs (crRNAs) were designed and used accordingly (Fig. 6A). Briefly, DNA-1 corresponds to a complementary strand of a well-established ATP aptamer in the literature (Xiong et al., 2020), while DNA-2 (sequence: 5′- CAT CTC AAT GGC AGG GGT GAG AAA T -3′) is a complementary DNA sequence of prostate cancer antigen 3, one of the most overexpressed genes in prostate cancer tissues and a biomarker that is excreted in patients' urine. Elevated DNA-2 levels during prostate cancer progression have made it a widely targeted biomarker for cancer detection (Nguyen et al., 2020). On the other hand, DNA-3 (sequence: 5′- CCG TGG TCG TCG ATT TTT TTT TTT T -3′) is a complementary DNA sequence of a reported copper-binding aptamer with chemical modification (Wang et al., 2024), while DNA-4 (sequence: 5′- GGG GCC GTC TTT TTT TGG CA -3′) is the complementary DNA sequence of a previously reported flunixin-binding aptamer (Chen et al., 2025). The experimental results were summarized in Fig. 6, with the LODs determined at 255 aM, 2.19 fM, 533 aM and 740 aM for DNA-1, DNA-2, DNA-3, and DNA-4, respectively (Fig. S15–18). Notably, these LODs represent at least a 100-fold improvement in the sensor sensitivity compared with previously reported amplification-free ssDNA detection methods.

3.6. Serum Sample Analysis

To evaluate the preliminary applicability of the developed CRISPR-Cas12a biosensor in a biological matrix, a human serum sample was analyzed using the procedure described in the Serum Sample Analysis section. Due to the significantly higher background fluorescence observed in serum compared with water, likely arising from intrinsic serum proteins as previously reported by Zhang and co-workers (Zhang et al., 2018), RNA was first extracted from 200 μL of serum prior to CRISPR-Cas12a analysis. No endogenous miRNA-21 was detected in the sample.

As a proof-of-concept assessment of matrix effects on assay performance, three mock serum samples were prepared by spiking miRNA-21 standard solutions into human serum at different concentrations and

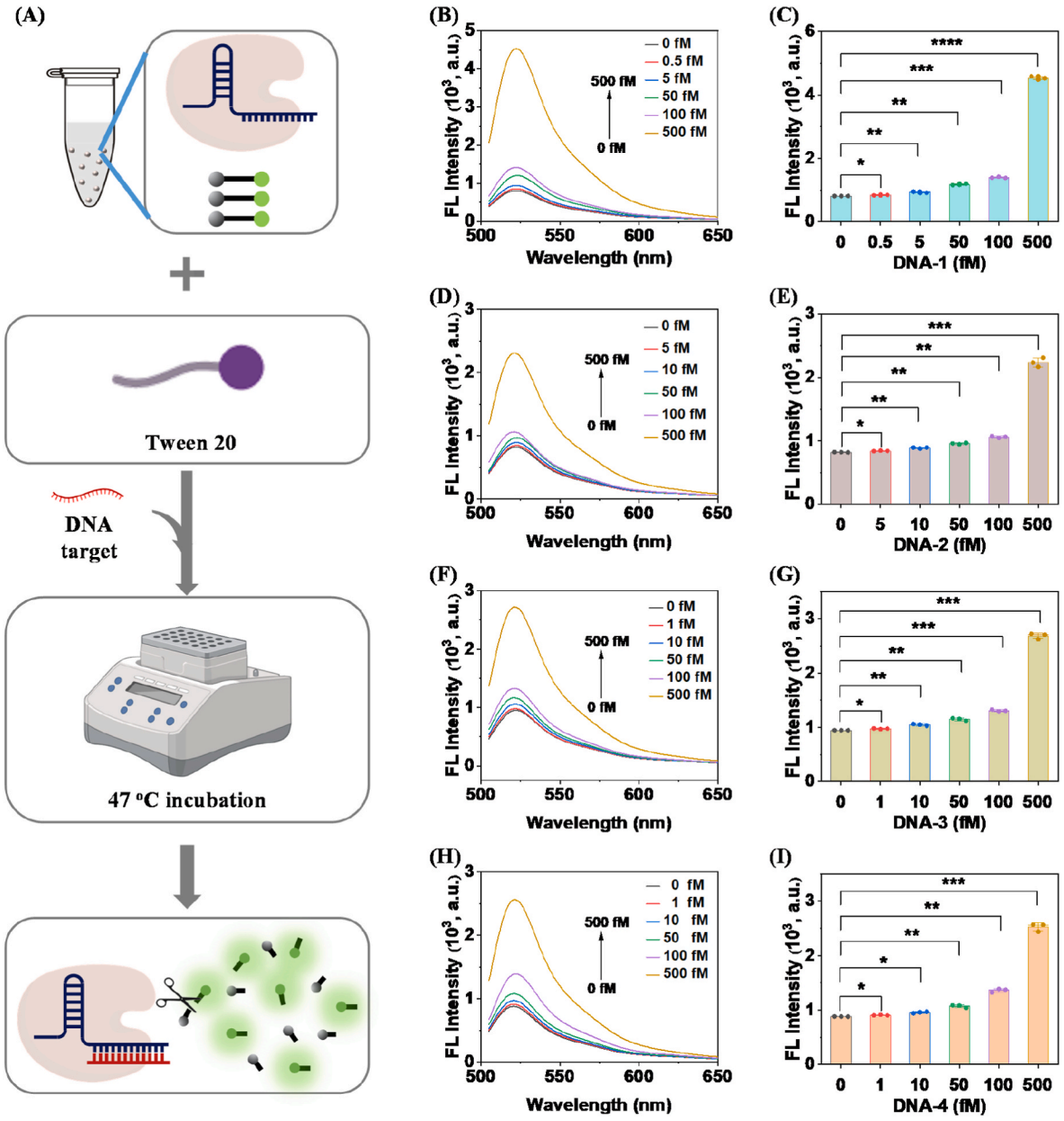


Fig. 6. Sensitivity studies of various DNA species. (A) Schematic representation of Tween 20-enhanced DNA detection by Cas12a. Fluorescence spectra of various DNA targets: (B) DNA-1; (D) DNA-2; (F) DNA-3; and (H) DNA-4, and the corresponding plots of the fluorescence intensity as a function of the analyte concentration: (C) DNA-1; (E) DNA-2; (G) DNA-3; and (I) DNA-4. The error bars indicate the average and standard deviation values derived from results obtained in three independent experiments (n = 3). Statistical analysis was conducted using a two-tailed *t*-test. Significance levels are indicated as follows: ns (not significant) for $P > 0.05$, * for $P < 0.05$, ** for $P < 0.01$, *** for $P < 0.001$, and **** for $P < 0.0001$. The incubation was performed at 47 °C for 3 h in DNA-optimized reaction medium.

analyzed following the same procedure. As summarized in Table 1, the developed CRISPR-Cas12a assay exhibited satisfactory analytical performance in the serum matrix, with recovery values ranging from 89% to 103%. These results demonstrate the feasibility of the proposed assay for RNA detection in complex biological samples. Nevertheless, because this study included only a limited number of serum samples, comprehensive validation using a larger cohort of clinical specimens will be the subject of future investigation.

Table 1
Simulated Human Serum Sample Analysis by Use of the CARD Sensor. Each experimental value represents the mean of three replicate analyses ± one standard deviation.

Sample Number	Theoretic Value (pM)	Experimental Value (pM)	Recovery (%)
1	2	1.78 ± 0.18	89.1 ± 9.3
2	5	4.81 ± 0.07	96.2 ± 1.5
3	10	10.31 ± 0.53	103.1 ± 5.3

4. Conclusion and future perspectives

In this study, we show that simple supplementation of the reaction buffer with Tween 20 and glycerol markedly enhances the sensitivity of the Cas12a-crRNA system for direct RNA detection. This CARD strategy enables femtomolar-level RNA quantification without the need for auxiliary components or nucleic acid amplification, thereby addressing a key limitation in CRISPR-based diagnostics—namely, the intrinsically weak RNA-triggered *trans*-cleavage activity of Cas12a. Compared with previously reported Cas12a-based RNA detection approaches, including

SAHARA, FCAS, PHD, and split-crRNA systems, CARD eliminates the requirement for DNA activators and avoids complex substrate engineering. Furthermore, in contrast to cascade-based designs such as asymmetric CRISPR and AutoCAR, this method offers a streamlined workflow with minimal design constraints, substantially simplifying experimental implementation. Notably, the incorporation of chemical additives also improves DNA detection sensitivity, lowering the LOD from the conventional picomolar to the attomolar range. This enhancement is likely attributed to increased *trans*-cleavage efficiency, suggesting that the additives enable more effective utilization of the intrinsic catalytic activity of Cas12a.

Despite these advances, several limitations warrant further investigation. First, the present study was limited to LbCas12a and AsCas12a, and it remains unclear whether similar chemical enhancement effects can be extended to other Cas12a orthologs or CRISPR-based systems. Second, the current platform has been validated only for nucleic acid targets of 20 nucleotides or longer, and further optimization of guide RNA design and reaction conditions will be required to enable efficient detection of shorter targets. Third, the assay currently requires approximately 3 h to complete. Future studies should systematically examine how Cas12a and crRNA concentrations influence the tradeoff between analytical sensitivity and assay duration to reduce detection time while maintaining low limits of detection. Finally, although substantial enhancement of *trans*-cleavage activity was observed, the molecular mechanism by which these additives modulate Cas12a function remains unclear and will require detailed biochemical and structural investigations. In addition, integrating the CARD strategy with amplification-free and rapid detection platforms may further improve sensitivity while shortening assay time, facilitating translation to high-throughput and point-of-care diagnostic applications.

CRediT authorship contribution statement

Jun Chen: Conceptualization, Data curation, Formal analysis, Investigation, Writing – original draft. **Haiyan Zheng:** Investigation. **Lucas Guan:** Investigation. **Anudha Kanaherarachchi:** Investigation. **Sathishkumar Munusamy:** Investigation. **Juanhua Kong:** Investigation. **Shuo Zhou:** Investigation. **Rana Jahani:** Investigation. **Xiyun Guan:** Conceptualization, Funding acquisition, Project administration, Resources, Supervision, Writing – review & editing.

Declaration of competing interest

The authors declare that they have no known competing financial interests or personal relationships that could have appeared to influence the work reported in this paper.

Acknowledgments

This work was financially supported by National Science Foundation (2345813).

Appendix A. Supplementary data

Supplementary data to this article can be found online at https://doi.org/10.1016/j.bios.2026.119048.

Data availability

Data will be made available on request.

References

Broughton, J.P., Deng, X., Yu, G., Fasching, C.L., Servellita, V., Singh, J., Miao, X., Streithorst, J.A., Granados, A., Sotomayor-Gonzalez, A., Zorn, K., Gopez, A., Hsu, E., Gu, W., Miller, S., Pan, C.Y., Guevara, H., Wadford, D.A., Chen, J.S., Chiu, C.Y., 2020. CRISPR-Cas12-based detection of SARS-CoV-2. Nat. Biotechnol. 38, 870–874. https://doi.org/10.1038/s41587-020-0513-4.

Cai, C., Qiu, X., Zeng, M., Lin, M., Lin, X., Lou, H., Zhan, X., Pang, Y., Huang, J., Xie, L., 2017. Using polyvinylpyrrolidone to enhance the enzymatic hydrolysis of lignocelluloses by reducing the cellulase non-productive adsorption on lignin. Bioresour. Technol. 227, 74–81. https://doi.org/10.1016/j.biortech.2016.12.002.

Chen, J., Munusamy, S., Jahani, R., Guan, R., Zheng, H., Zhou, S., Kong, J., Zhao, Y., Guan, L., Kanaherarachchi, A., Guan, X., 2025. Cooperative split DNA activation of CRISPR-Cas12a for sensitive and selective detection of flunixin. ACS Meas. Sci. Au 5, 942–950. https://doi.org/10.1021/acsmeasuresciau.5c00114.

Chen, J.S., Ma, E., Harrington, L.B., Da Costa, M., Tian, X., Palefsky, J.M., Doudna, J.A., 2018. CRISPR-Cas12a target binding unleashes indiscriminate single-stranded DNase activity. Science 360, 436–439. https://doi.org/10.1126/science.aar6245.

Chen, X., Zhou, S., Wang, Y., Zheng, L., Guan, S., Wang, D., Wang, L., Guan, X., 2023. Nanopore single-molecule analysis of biomarkers: providing possible clues to disease diagnosis. Trends Anal. Chem. 162, 117060. https://doi.org/10.1016/j.trac.2023.117060.

Chen, Y., Wang, X., Zhang, J., Jiang, Q., Qiao, B., He, B., Yin, W., Qiao, J., Liu, Y., 2024. Split crRNA with CRISPR-Cas12a enabling highly sensitive and multiplexed detection of RNA and DNA. Nat. Commun. 15, 8342. https://doi.org/10.1038/s41467-024-52691-x.

Deng, F., Li, Y., Li, B., Goldys, E.M., 2022. Increasing trans-cleavage catalytic efficiency of Cas12a and Cas13a with chemical enhancers: application to amplified nucleic acid detection. Sens. Actuators, B Chem. 373, 132767. https://doi.org/10.1016/j.snb.2022.132767.

Deng, F., Li, Y., Yang, B., Sang, R., Deng, W., Kansara, M., Lin, F., Thavaneswaran, S., Thomas, D.M., Goldys, E.M., 2024. Topological barrier to Cas12a activation by circular DNA nanostructures facilitates autocatalysis and transforms DNA/RNA sensing. Nat. Commun. 15, 1818. https://doi.org/10.1038/s41467-024-46001-8.

Fei, X., Lei, C., Ren, W., Liu, C., 2025. 'Splice-at-will' Cas12a crRNA engineering enabled direct quantification of ultrashort RNAs. Nucleic Acids Res. 53. https://doi.org/10.1093/nar/gkaf002.

Feng, W., Peng, H., Xu, J., Liu, Y., Pabbaraju, K., Tipples, G., Joyce, M.A., Saffran, H.A., Tyrrell, D.L., Babiuk, S., Zhang, H., Le, X.C., 2021. Integrating reverse transcription recombinase polymerase amplification with CRISPR technology for the one-tube assay of RNA. Anal. Chem. 93, 12808–12816. https://doi.org/10.1021/acs.analchem.1c03456.

Feng, Z.Y., Yun, Y.F., Li, X., Zhang, J., 2023. Impact of divalent metal ions on regulation of trans-cleavage activity of CRISPR-Cas13a: a combined experimental and computational study. Chembiochem 24, e202300034. https://doi.org/10.1002/cbic.202300034.

Gorski, S.A., Vogel, J., Doudna, J.A., 2017. RNA-based recognition and targeting: sowing the seeds of specificity. Nat. Rev. Mol. Cell Biol. 18, 215–228. https://doi.org/10.1038/nrm.2016.174.

Hu, Z., Ling, S., Duan, J., Yu, Z., Che, Y., Wang, S., Zhang, S., Zhang, X., Li, Z., 2025. Proximity-activated guide RNA of CRISPR-Cas12a for programmable diagnostic detection and gene regulation. Nucleic Acids Res. 53. https://doi.org/10.1093/nar/gkaf017.

Jiang, Q., Jin, S., Qin, Z., Zhang, J., He, R., Chen, Z., Qiao, B., Qiao, J., Liu, Y., 2025. CRISPR/Cas12a DTR system: a topology-guided Cas12a assay for specific dual detection of RNA and DNA targets. Nucleic Acids Res. 53. https://doi.org/10.1093/nar/gkaf893.

Jiao, C., Sharma, S., Dugar, G., Peeck, N.L., Bischler, T., Wimmer, F., Yu, Y., Barquist, L., Schoen, C., Kurzai, O., Sharma, C.M., Beisel, C.L., 2021. Noncanonical crRNAs derived from host transcripts enable multiplexable RNA detection by Cas9. Science 372, 941–948. https://doi.org/10.1126/science.abe7106.

Kaminski, M.M., Abudayyeh, O.O., Gootenberg, J.S., Zhang, F., Collins, J.J., 2021. CRISPR-based diagnostics. Nat. Biomed. Eng. 5, 643–656. https://doi.org/10.1038/s41551-021-00760-7.

Kim, H., Lee, W.J., Oh, Y., Kang, S.H., Hur, J.K., Lee, H., Song, W., Lim, K.S., Park, Y.H., Song, B.S., Jin, Y.B., Jun, B.H., Jung, C., Lee, D.S., Kim, S.U., Lee, S.H., 2020. Enhancement of target specificity of CRISPR-Cas12a by using a chimeric DNA-RNA guide. Nucleic Acids Res. 48, 8601–8616. https://doi.org/10.1093/nar/gkaa605.

Li, J., Luo, T., He, Y., Liu, H., Deng, Z., Bu, J., Long, X., Zhong, S., Yang, Y., 2022. Discovery of the Rnase activity of CRISPR-Cas12a and its distinguishing cleavage efficiency on various substrates. Chem. Commun. 58, 2540–2543. https://doi.org/10.1039/d1cc06295f.

Li, M.Y., Niu, H., Jiang, J., Wu, X.Y., Ying, Y.L., Long, Y.T., 2025. Real-time recording the dynamic catalytic heterogeneity of enzymatic reactions using a nanopore. J. Am. Chem. Soc. 147, 17121–17131. https://doi.org/10.1021/jacs.5c02535.

Li, S.Y., Cheng, Q.X., Wang, J.M., Li, X.Y., Zhang, Z.L., Gao, S., Cao, R.B., Zhao, G.P., Wang, J., 2018. CRISPR-Cas12a-assisted nucleic acid detection. Cell Discov. 4, 20. https://doi.org/10.1038/s41421-018-0028-z.

Li, Z., Zhao, W., Ma, S., Yao, Y., Fei, T., 2021. A chemical-enhanced system for CRISPR-based nucleic acid detection. Biosens. Bioelectron. 192, 113493. https://doi.org/10.1016/j.bios.2021.113493.

Lin, M., Yue, H., Tian, T., Xiong, E., Zhu, D., Jiang, Y., Zhou, X., 2022. Glycerol additive boosts 100-fold sensitivity enhancement for one-pot RPA-CRISPR/Cas12a assay. Anal. Chem. 94, 8277–8284. https://doi.org/10.1021/acs.analchem.2c00616.

Liu, P., Zeng, J., Jiang, C., Du, J., Jiang, L., Li, S., Zeng, F., Xiong, E., 2024. Poly (vinylpyrrolidone)-enhanced CRISPR-cas system for robust nucleic acid diagnostics. Anal. Chem. 96, 15797–15807. https://doi.org/10.1021/acs.analchem.4c04077.

Ma, P., Meng, Q., Sun, B., Zhao, B., Dang, L., Zhong, M., Liu, S., Xu, H., Mei, H., Liu, J., Chi, T., Yang, G., Liu, M., Huang, X., Wang, X., 2020. MeCas12a, a highly sensitive and specific system for COVID-19 detection. Adv. Sci. 7, 2001300. https://doi.org/10.1002/advs.202001300.

Moon, J., Zhang, J., Guan, X., Yang, R., Guo, C., Schalper, K.T., Avery, L., Banach, D., LaSala, R., Warrier, R., Liu, C., 2025. CRISPR anti-tag-mediated room-temperature RNA detection using CRISPR/Cas13a. Nat. Commun. 16, 9142. https://doi.org/10.1038/s41467-025-64205-4.

Munusamy, S., Zheng, H., Chen, J., Zhou, S., Kong, J., Jahani, R., Zhao, Y., Guan, X., 2025. Gold nanoparticle-assisted CRISPR-Cas12a-Based activity assay for highly sensitive detection of trypsin. ACS Appl. Bio Mater. 8, 6379–6387. https://doi.org/10.1021/acsabm.5c00854.

Nguyen, L.T., Rananaware, S.R., Pizzano, B.L.M., Stone, B.T., Jain, P.K., 2022. Clinical validation of engineered CRISPR/Cas12a for rapid SARS-CoV-2 detection. Commun. Med. 2, 7. https://doi.org/10.1038/s43856-021-00066-4.

Nguyen, L.T., Smith, B.M., Jain, P.K., 2020. Enhancement of trans-cleavage activity of Cas12a with engineered crRNA enables amplified nucleic acid detection. Nat. Commun. 11, 4906. https://doi.org/10.1038/s41467-020-18615-1.

Qiao, J., Zhang, J., Jiang, Q., Jin, S., He, R., Qiao, B., Liu, Y., 2025. Boosting CRISPR/Cas12a intrinsic RNA detection capability through pseudo hybrid DNA-RNA substrate design. Nucleic Acids Res. 53. https://doi.org/10.1093/nar/gkaf510.

Qing, M., Huang, C., Li, Y., Yu, Q., Hu, Q., Zhou, J., Yuan, R., Bai, L., 2025. Dithiothreitol facilitates LbCas12a with expanded PAM preference for ultrasensitive nucleic acid detection. Anal. Chem. 97, 6286–6294. https://doi.org/10.1021/acs.analchem.5c00280.

Rananaware, S.R., Vesco, E.K., Shoemaker, G.M., Anekar, S.S., Sandoval, L.S.W., Meister, K.S., Macaluso, N.C., Nguyen, L.T., Jain, P.K., 2023. Programmable RNA detection with CRISPR-Cas12a. Nat. Commun. 14, 5409. https://doi.org/10.1038/s41467-023-41006-1.

Rossetti, M., Merlo, R., Bagheri, N., Moscone, D., Valenti, A., Saha, A., Arantes, P.R., Ippodrino, R., Ricci, F., Treglia, I., Delibato, E., van der Oost, J., Palermo, G., Perugino, G., Porchetta, A., 2022. Enhancement of CRISPR/Cas12a trans-cleavage activity using hairpin DNA reporters. Nucleic Acids Res. 50, 8377–8391. https://doi.org/10.1093/nar/gkac578.

Sun, W., Xiao, Y., Wang, K., Zhang, S., Yao, L., Li, T., Cheng, B., Zhang, P., Huang, S., 2025. Nanopore discrimination of rare earth elements. Nat. Nanotechnol. 20, 523–531. https://doi.org/10.1038/s41565-025-01864-w.

Swarts, D.C., van der Oost, J., Jinek, M., 2017. Structural basis for guide RNA processing and seed-dependent DNA targeting by CRISPR-Cas12a. Mol. Cell 66, 221–233. https://doi.org/10.1016/j.molcel.2017.03.016.

Swarts, D.C., Jinek, M., 2019. Mechanistic insights into the cis- and trans-Acting DNase activities of Cas12a. Mol. Cell 73, 589–600. https://doi.org/10.1016/j.molcel.2018.11.021.

Wang, J., Liu, Y., Li, X., Lei, H., Liu, J., 2024. A high affinity and selective DNA aptamer for copper ions. Chem. Commun. 60, 14272–14275. https://doi.org/10.1039/d4cc05410e.

Wang, X., Qin, Y., Huang, Y., Hu, K., Zhao, S., Tian, J., 2022. A sensitive and facile microRNA detection based on CRISPR-Cas12a coupled with strand displacement amplification. Spectrochim. Acta Mol. Biomol. Spectrosc. 279, 121476. https://doi.org/10.1016/j.saa.2022.121476.

Xiong, Y., Zhang, J., Yang, Z., Mou, Q., Ma, Y., Lu, Y., 2020. Functional DNA regulated CRISPR-Cas12a sensors for point-of-care diagnostics of non-nucleic-acid targets. J. Am. Chem. Soc. 142, 207–213. https://doi.org/10.1021/jacs.9b09211.

Yi, Y., Song, P., Li, Z., Ju, J., Sun, G., Ren, Q., Zhou, K., Liu, L., Wu, H.C., 2025. Nanopore-based enzyme-linked immunosorbent assay for cancer biomarker detection. Nat. Nanotechnol. 20, 1079–1086. https://doi.org/10.1038/s41565-025-01918-z.

Zetsche, B., Abudayyeh, O.O., Gootenberg, J.S., Scott, D.A., Zhang, F., 2020. A survey of genome editing activity for 16 Cas12a orthologs. Keio J. Med. 69, 59–65. https://doi.org/10.2302/kjm.2019-0009-OA.

Zhang, J., Li, Z., Guo, C., Guan, X., Avery, L., Banach, D., Liu, C., 2024. Intrinsic RNA targeting triggers indiscriminate DNase activity of CRISPR-Cas12a. Angew. Chem. Int. Ed. 63, e202403123. https://doi.org/10.1002/anie.202403123.

Zhang, J., Yin, W., Jiang, Q., Mao, W., Deng, W., Jin, S., Wang, X., He, R., Qiao, J., Liu, Y., 2025. Precise amplification-free detection of highly structured RNA with an enhanced SCas12a assay. Commun. Biol. 8, 366. https://doi.org/10.1038/s42003-025-07806-5.

Zhang, W.S., Pan, J., Li, F., Zhu, M., Xu, M., Zhu, H., Yu, Y., Su, G., 2021a. Reverse transcription recombinase polymerase amplification coupled with CRISPR-Cas12a for facile and highly sensitive colorimetric SARS-CoV-2 detection. Anal. Chem. 93, 4126–4133. https://doi.org/10.1021/acs.analchem.1c00013.

Zhang, Y., Chen, X., Roozbahani, G.M., Guan, X., 2018. Graphene oxide-based biosensing platform for rapid and sensitive detection of HIV-1 protease. Anal. Bioanal. Chem. 410, 6177–6185. https://doi.org/10.1007/s00216-018-1224-2.

Zhang, Y., Ren, Q., Tang, X., Liu, S., Malzahn, A.A., Zhou, J., Wang, J., Yin, D., Pan, C., Yuan, M., Huang, L., Yang, H., Zhao, Y., Fang, Q., Zheng, X., Tian, L., Cheng, Y., Le, Y., McCoy, B., Franklin, L., Selengut, J.D., Mount, S.M., Que, Q., Qi, Y., 2021b. Expanding the scope of plant genome engineering with Cas12a orthologs and highly multiplexable editing systems. Nat. Commun. 12, 1944. https://doi.org/10.1038/s41467-021-22330-w.

Zhao, Q., de Zoysa, R.S., Wang, D., Jayawardhana, D.A., Guan, X., 2009. Real-time monitoring of peptide cleavage using a nanopore probe. J. Am. Chem. Soc. 131, 6324–6325. https://doi.org/10.1021/ja9004893.

Zhao, S., Zhang, Q., Luo, R., Sun, J., Zhu, C., Zhou, D., Gong, X., 2024. Amplification-free miRNA detection with CRISPR/Cas12a system based on fragment complementary activation strategy. Chem. Sci. 15, 18347–18354. https://doi.org/10.1039/d4sc05647g.

Zheng, H., Munusamy, S., Arora, P., Jahani, R., Guan, X., 2024. A highly sensitive nanopore platform for measuring RNase A activity. Talanta 276, 126276. https://doi.org/10.1016/j.talanta.2024.126276.

Zheng, H., Munusamy, S., Kong, J., Kanaherarachchi, A., Zhou, S., Chen, J., Jahani, R., Guan, X., 2026a. Nanopore label-free monitoring of B-DNA and Z-DNA conformational transition in real time. ACS Nano 20, 5208–5216. https://doi.org/10.1021/acsnano.5c20616.

Zheng, H., Munusamy, S., Zhou, S., Jahani, R., Chen, J., Kong, J., Guan, X., 2025. Nanopore detection of small molecules based on replacement and complexation chemical interactions. Small 21, e2407184. https://doi.org/10.1002/smll.202407184.

Zheng, H., Munusamy, S., Zhou, S., Kanaheraarachchi, A., Kong, J., Chen, J., Jahani, R., Zhao, Y., Guan, X., 2026b. Label-free nanopore determination of the binding mode, kinetics and thermodynamics of DNA-drug interactions. Small Methods 10, e01003. https://doi.org/10.1002/smtd.202501003.